Synthetic Approaches for Accessing Rare-Earth Analogues of UiO-66

P. Rafael Donnarumma,[1] Sahara Frojmovic,[1] Hudson de Aguiar Bicalho,[1] Hatem M. Titi,[2] Ashlee J. Howarth*[1]

[1]Department of Chemistry and Biochemistry, and Centre for NanoScience Research, Concordia University, 7141 Sherbrooke St W., Montréal, QC, H4B 1R6

[2] Department of Chemistry, McGill University, 801 Sherbrooke St W., Montréal, QC, H3A 0B8

Abstract:

Rare-earth (RE) analogues of UiO-66 with non-functionalised 1,4-benzenedicarboxylate linkers are synthesised for the first time, and a series of synthetic approaches is provided to troubleshoot the synthesis. RE-UiO-66 analogues are fully characterised, and demonstrate a high degree of crystallinity, high surface area and thermal stability, consistent with the UiO-66 archetype.

Introduction

Metal–organic frameworks (MOFs) are a family of structurally diverse and porous materials constructed *via* the concatenation of metal ions, or clusters, with organic ligands, known as linkers, extending in 2- or 3-dimensions.[1,2] These inorganic and organic building units act as nodes and vertices in a topological net, ciphered according to Reticular Chemistry Structure Resource (RCSR) by a three-letter code, such as **bct**, **fcu** or **spn**, representing the uniqueness of that net's connectivity.[3] Through the use of reticular chemistry as a design strategy, MOFs with specific properties and architectures (or nets), can be built by carefully selecting the inorganic and organic building units, also known as secondary building units (SBUs), that will constitute it.[4,5] The properties of the MOF, dictated in part by the choice of SBUs, will thus determine its potential in applications, within which catalysis,[6–9] gas adsorption,[10–12] chemical sensing,[13,14] water treatment,[15–17] and many more can be found.[18–22]

Among the various MOF families, Zr-based MOFs have been extensively studied due to their high stability, Lewis acidity, and structural tunability, making them attractive for diverse applications. In particular, there is a substantial amount of interest in Zr-MOFs containing the hexanuclear metal-oxide cluster, $[Zr_6O_4(OH)_4]^{12+}$, as an SBU[23–25] with the most well-known and well-studied example being Zr-UiO-66.[26] Zr-UiO-66 is comprised of 12-connected (12-c) Zr-hexanuclear clusters bridged together by 1,4-benzenedicarboxylate (BDC), a 2-c linker, giving rise to a 12,2-c (also known as just 12-c) **fcu** net.[23,27] To this day, Zr-UiO-66 and its diverse analogues and derivatives have been studied for several different applications.[26] Focusing on the inorganic component alone, several tetravalent ions have been used in the syntheses of isostructural BDC-containing analogues M-UiO-66 (M = Hf(IV), Ce(IV), Th(IV), U(IV), Pu(IV) and Np(IV)).[26]

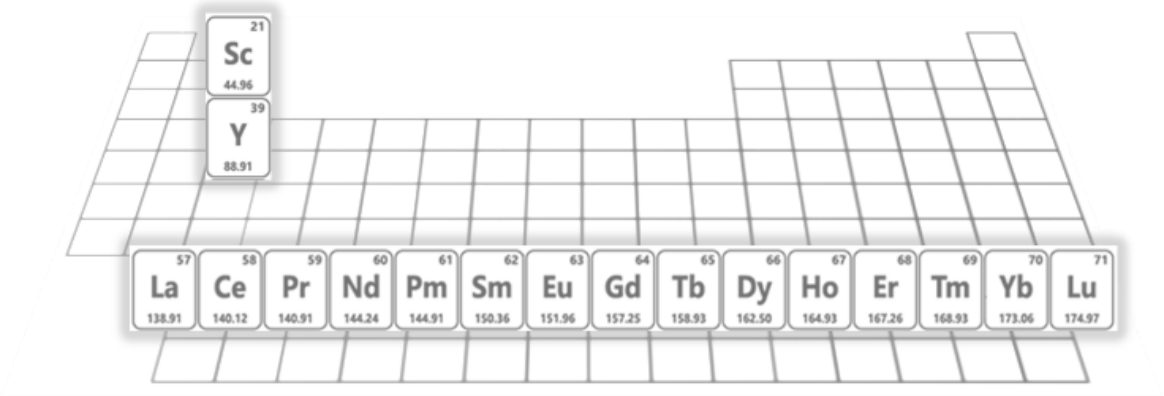

Figure 1. Periodic table schematic highlighting the rare-earth elements.

Another intriguing family of MOFs with diverse structures and properties are those comprised of rare-earth (RE) elements.[28] RE elements include the 15 lanthanoids from the *f*-block plus Y and Sc (**Figure 1**). The RE metals located in the *f*-block possess unique electronic properties dictated by their 4f electron configuration, allowing RE-MOFs to be explored for magnetic and optoelectronic applications, in addition to the traditionally studied applications of MOFs.[29] Using RE(III) ions to form inorganic SBUs, a vast library of MOFs has been developed, many with unique structures and topologies that result from the variability in the coordination environment of RE(III) ions.[20,30–33] Much like other MOFs, RE-MOFs with different types of inorganic SBUs have been reported, including single ion-,[34–36] chain-,[37,38] or cluster-based SBUs.[39–41] Similar to tetravalent ions, RE(III) ions can be used to construct hexanuclear clusters that are structurally similar to that of Zr-UiO-66.[12,42] Eddaoudi *et al.* demonstrated that the synthesis of these hexanuclear RE-clusters is possible by using alpha-fluorinated acids as modulators.[30] As such, these clusters have been used to synthesise a handful of RE-MOFs, some of them isostructural to Zr-UiO-66 with functionalised linkers.[42–44] However, to this date, RE-UiO-66 analogues, with non-functionalised BDC linkers, have not been reported in literature. Herein, we present the synthesis and characterization of a series of isostructural RE-UiO-66 analogues (**Figure 2**) prepared from the commercially available, and cost-effective BDC linker. The resulting new family of RE-MOFs, RE-UiO-66 (RE = Y, Eu, Gd, Tb, Ho, Er, Tm, Yb),[45] exhibits both high surface area and good thermal stability. Furthermore, we provide alternatives to troubleshoot the synthesis since its reproducibility can be challenging due to solvent quality. This synthesis of RE-analogues of UiO-66 will allow for the addition of RE-UiO-66 to the MOF repertoire.

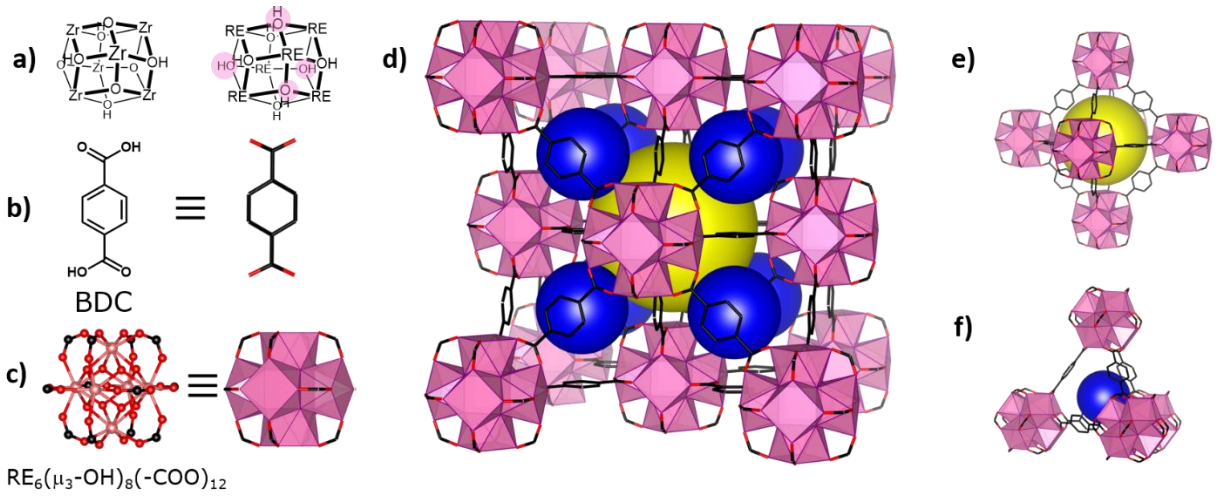

Figure 2. Structure of RE-UiO-66. (a) Differences between Zr- and RE-hexanuclear cluster highlighted in pink. (b) Linear 1,4-benzenedicarboxylate (BDC) linkers will connect the (c) 12-c SBU to establish (d) RE-UiO-66 with **fcu** topology. Two kind of cages exist in the net, (e) the octahedral cage (yellow sphere), and (f) the tetrahedral cages (blue spheres).

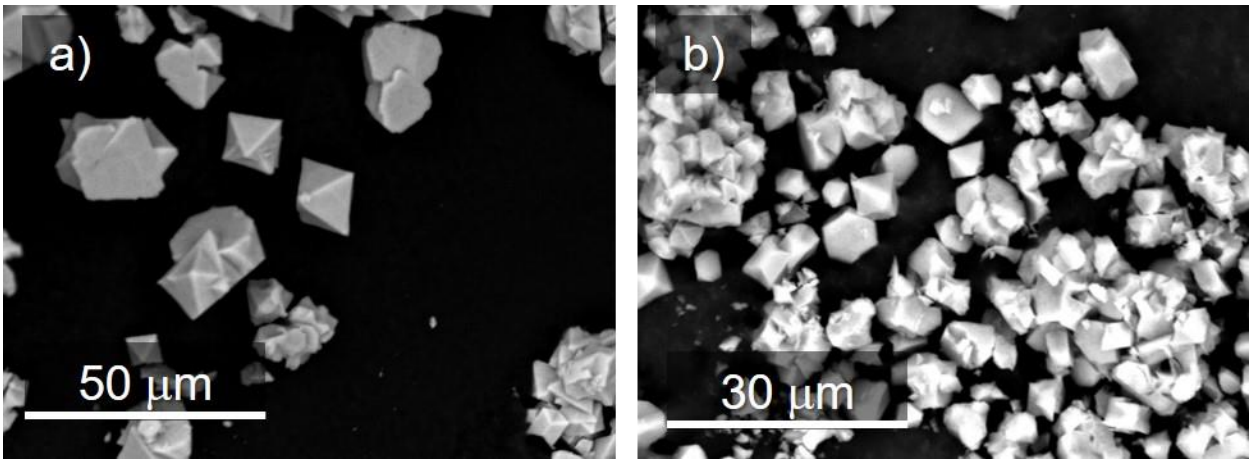

Figure 3. SEM showing the polyhedral crystals for: (a) Tm-UiO-66 and (b) Y-UiO-66 (right).

Result and Discussion

Solvothermal reactions between $RE(NO_3)_3 \cdot xH_2O$ (RE = Y, Eu, Gd, Tb, Ho, Er, Tm, Yb) and BDC in different N,N'-dimethylformamide (DMF)/N,N'-dimethylacetamide (DMA) solvent mixtures in the presence of 2,6-difluorobenzoic acid (2,6-DFBA) yield transparent, homogeneous, and polyhedral crystals corresponding to RE-UiO-66 (RE = Y, Eu, Gd, Tb, Ho, Er, Tm, Yb) (**Figure 3**). Initially, synthetic conditions for the precipitation of RE-UiO-66 were screened for Y-UiO-66, after which the conditions were adapted to obtain the rest of the series. Of these, Tm-UiO-66 synthesised in DMA in the presence of HCl, produced crystals large enough (ca. 80 μm) for single-crystal X-ray diffraction (SCXRD), which indicated the following formula: $[(CH_3)_2NH_2]_2[Tm_6(\mu_3\text{-}OH)_8(BDC)_6].(DMA)_6.(H_2O)_3$ (see SI for detail). Unlike M(IV) analogues of UiO-66, RE(III)-UiO-66 is anionic in nature, $[RE_6(\mu_3\text{-}OH)_8(BDC)_6]^{2-}$, and the charge must be compensated with counterions to achieve charge neutrality. Both in DMF and in DMA solutions,

$[(CH_3)_2NH_2]^+$ can be found as a product of decomposition at high temperatures, providing the cation necessary for balancing the anionic MOF. The phase purity of the RE-UiO-66 series was confirmed by comparison to the calculated powder X-ray diffraction pattern (PXRD) obtained from the single crystal data of Tm-UiO-66, and all materials are confirmed to be isostructural to Zr-UiO-66 (**Figure 4**). The lattice parameter for Zr-UiO-66 is 20.7 Å, whereas it is 21.2 Å for Tm-UiO-66, an expected increase based on the differences in ionic radius for Zr(IV) (0.84 Å, coordination number: 8) and Tm(III) (0.99 Å, coordination number: 8). A topological analysis of Tm-UiO-66 corroborated its topology as **fcu** assembled from 12-c $[Tm_6(\mu_3\text{-}OH)_8(O_2C\text{-})_{12}]^{2-}$ SBUs, wherein the carbon in the carboxylic acid acts as a point of extension. Analogous to M(IV)-UiO-66, RE-UiO-66 contains two types of cages: an octahedral cage located at the centre of the unit cell and face-sharing with 8 tetrahedral cages (**Figure 2e and 2f**). The diameters of these cages are found to be ca. 12 Å and ca. 7 Å, respectively accessible through triangular windows with apertures of ca. 6 Å.

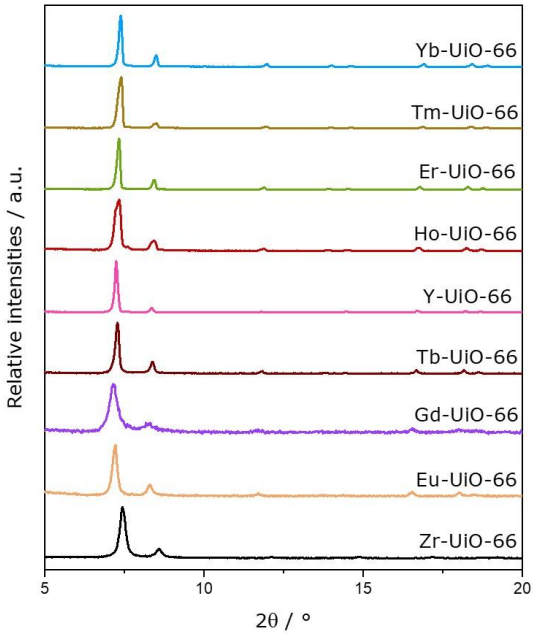

Figure 4. Stacked PXRDs for all the as-synthesised RE-UiO-66 analogues and Zr-UiO-66 for comparison. The peaks are collected up to 20° 2theta alone since the characteristic peaks for UiO-66 are found in this range.

After several synthetic attempts, optimised conditions were found to synthesize RE-UiO-66 (RE = Y, Ho, Er, Tm, Yb) using DMF as the reaction solvent. This procedure, however, could not be translated to Eu, Gd, or Tb, which gave low quality, impure and/or completely different materials. DMF is the most widely used solvent for MOF synthesis, owing in part to its high boiling point, polar aprotic nature, and hydrolytic decomposition to give dimethylamine (a base that can aid with deprotonation of carboxylic acid linkers) and formate (a ligand that can cap and stabilize inorganic SBUs).[47] DMA is a solvent with similar properties, albeit with a slower rate of decomposition to yield dimethylamine and acetate at high temperatures under acidic conditions.[47] As such, we explored the use of DMA for the synthesis of RE-UiO-66, in an attempt to modify the linker deprotonation process. Interestingly, the Eu and Tb analogues, as well as the others

previously obtained in DMF, were obtained using DMA as the solvent. Given that DMA is significantly more expensive than DMF,[47] we sought to optimize the procedure using the minimum necessary amount of DMA. It should be noted that in order to precipitate materials of appreciable quality, different mixtures of DMF/DMA are required. Specifically, a ratio of 7:1 (DMA:DMF) is needed for Eu-UiO-66, 3:5 for Gd-UiO-66, while 1:7 is enough for Tb-UiO-66. Coincidentally, the three RE-UiO-66 analogues that require the presence of this auxiliary solvent to form, Eu, Gd and Tb, are the ones with the largest ionic radii in the series. This suggests that a more sterically bulky solvent with a slower decomposition rate may be required when RE-UiO-66 comprised of ions with larger ionic radii is desired.

On the other hand, the formation of RE-UiO-66 (RE = Y, Ho, Er, Tm and Yb) in DMF was found to be susceptible to variability between sources of DMF, where batches coming from different, or even the same, commercial sources give different results (**Figure S1**). This reproducibility issue can be solved by replacing some of the DMF in the reaction mixture with DMA, but since the objective was to keep the amount of DMA to a minimum, a screening of different monoprotic acids (HCl and HNO_3) was performed. It was found that a ratio of 160:1 of DMF to HNO_3 was sufficient to allow for the formation of RE-UiO-66, without the addition of DMA, in instances where DMF resulted in impure samples. Owing to our observations, which include results from testing over 100 reaction conditions, we have outlined a series of steps to troubleshoot the reaction conditions if RE-UiO-66 is the desired product:

1. Follow the reaction as it is described in the SI, using DMF as the solvent
2. If the product shows impurities (**Figure S1**), add HNO_3 in a 160:1 ratio (DMF:HNO_3) (for RE = Y, Ho, Er, Tm, Yb) (**Figure S2**)
3. If the addition of HNO_3 cannot be adjusted to form a pure material, replace DMF with DMA (**Figure S3**), either partially or completely (for RE = Y, Eu, Gd, Tb, Ho, Er, Tm, Yb, (see SI for details). This synthesis procedure is highly robust and reproducible.

Previous reports have shown the utility of 2-fluorobenzoic acid (2-FBA) as a modulator for the generation of the hexanuclear RE-cluster SBU, as well as other lower and higher nuclearity RE-clusters.[28] Although 2-FBA has been used to synthesise some RE-UiO-66 isostructures in DMF,[12,43] in our hands, and using BDC as a linker, it did not yield the target RE-UiO-66 in a solution containing DMF. Other fluorinated modulators, including trifluoroacetic acid and other fluoro-substituted benzoic acid derivatives were thus explored under various conditions. Only 2,6-DFBA was found to be a successful modulator for obtaining the desired material when using DMF as the solvent. It was found nonetheless that 2-FBA in combination with DMA can yield Y-UiO-66 (**Figure S4**).

To confirm the surface area and porosity of the RE-UiO-66 series, various activation procedures were attempted, and N_2 adsorption/desorption analysis was performed. After exposure of Y-UiO-66 to several activation conditions (**Table S1**), it was found that an activation temperature of 80 °C for a time lapse of 20 h under vacuum was sufficient to activate the material and obtain a surface area comparable to that reported for Zr-UiO-66 (ca. 1200 m^2/g).[48] N_2 adsorption/desorption measurements on RE-UiO-66 (RE = Y, Eu, Tb, Er, Tm, Yb) analogues activated at 80 °C (**Figure 5**) show Type-I isotherms, expected for UiO-66 isostructural materials, with apparent Brunauer-Emmet-Teller (BET) surface areas (SAs) and pore volumes of 1360 m^2/g and 0.56 cm^3/g (Y), 890 m^2/g and 0.36 cm^3/g (Eu), 1030 m^2/g and 0.43 cm^3/g (Tb), 1190 m^2/g and 0.49 cm^3/g Er), 1010 m^2/g and 0.42 cm^3/g (Tm), and 1080 m^2/g and 0.43 cm^3/g (Yb). Differences in BET SA between RE-UiO-66 analogues can be attributed to the variable atomic mass of the RE-elements, quality of material (in the case of Eu), and due to the fact that activation procedures were only optimized for Y-UiO-66 and then applied to the rest of the RE-UiO-66 series. In addition, pore size distribution analysis by non-local density functional theory (NLDFT) reveals that the octahedral pores have diameters of ca. 10 Å for the entire series. To our surprise, upon revaluation of the N_2 isotherm for Y-UiO-66, 2 to 3

days after the initial measurement, the isotherm was changed, and the BET SA was reduced significantly, eventually reaching a value of 0 m²/g after 7 days. Given that such a reduction in SA is likely to be accompanied by a loss of crystallinity, PXRD measurements were collected 2 to 7 days post activation for all materials, showing a loss in crystallinity, corresponding to a decrease in reflection intensity of 60-90% after two days (**Figure S5a**). Similarly, when the solvent exchanged Y-UiO-66 was left under ambient conditions in a capped vial for more than 40 days a reduction can be observed as well (**Figure S5b**). Contrary to what is observed for Zr-UiO-66, activation of RE-UiO-66 appears to lead to its degradation or collapse a short time after the process. We hypothesise that removal of $(CH_3)_2NH_2^+$ during activation might be occurring, and thus, it is affecting the stability of the framework. Further research is being done in this respect.

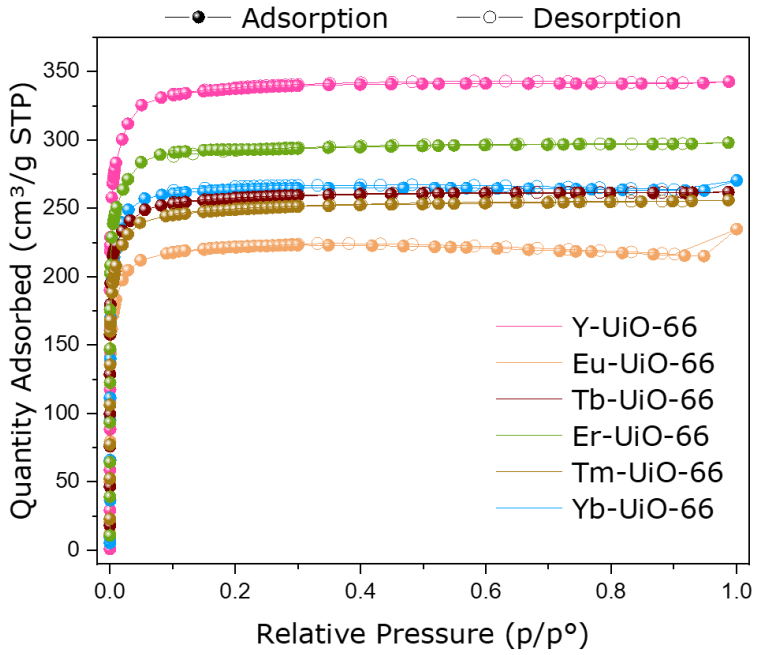

Figure 5. Nitrogen adsorption-desorption isotherms for RE-UiO-66 (RE = Y, Eu, Tb, Er, Tm, Yb).

The thermal stability of RE-UiO-66 (RE = Y, Eu, Tb, Er, Tm, Yb) was investigated through thermogravimetric analysis (TGA) on activated samples (**Figure S6**) under air. In all cases, the thermogram shows a loss in mass due to the loss of moisture below 100 °C, followed by a major mass loss ca. 500 °C. Eu-UiO-66 shows a slightly different thermogram than the rest of the RE-UiO-66 series and it decomposes at a lower temperature (450 °C vs 500 °C). This is likely due to the fact that Eu^{3+}, the weakest Lewis acid from the series, makes the Eu-O bond more labile. Analysis of the residue mass % (assumed to be RE_2O_3), as well as inductively coupled plasma mass spectrometry (ICP-MS) data (see SI for details) suggest that all RE-UiO-66 analogues contain some defects (i.e, missing linkers or missing nodes) in their structure, similar to what is observed for Zr-UiO-66.[48–50] Additionally, variable temperature (VT) PXRD was performed on non-activated Y-UiO-66 to corroborate that no major changes in the structure are occurring upon heating (**Figure S7**). Indeed, Y-UiO-66 does not undergo major changes or loss of crystallinity when heated up to 200 °C. This highlights the thermal stability of the material pre-activation, being comparable to that of Zr-UiO-66.[27]

Conclusions

We report here the synthesis and characterisation of a family of RE-UiO-66 (RE = Y, Eu, Gd, Tb, Ho, Er, Tm, Yb). This series of RE-UiO-66 materials are analogues of the archetypical Zr-UiO-66, synthesized using BDC with RE-metals for the first time. We provide a series of steps that can be taken to obtain the various RE-UiO-66 analogues, in the event that solvent quality affects the reproducibility of the synthetic protocol. RE-UiO-66 (RE = Y, Eu, Tb, Er, Tm, Yb) demonstrates permanent porosity with a range of surface areas from 890 to 1370 m^2/g. It was found that after activation the material tends to degrade with time and currently this phenomenon is being studied in more detail. However, pre-activation these MOFs demonstrate high thermal stability with VT-PXRD of Y-UiO-66 showing that there are no phase transitions or notable decomposition in the range of 25 °C – 200 °C.

References

1 S. R. Batten, N. R. Champness, X.-M. Chen, J. Garcia-Martinez, S. Kitagawa, L. Öhrström, M. O'Keeffe, M. P. Suh and J. Reedijk, *CrystEngComm*, 2012, **14**, 3001–3004.
2 S. R. Batten, N. R. Champness, X.-M. Chen, J. Garcia-Martinez, S. Kitagawa, L. Öhrström, M. O'Keeffe, S. M. Paik and J. Reedijk, *Pure Appl. Chem.*, 2013, **85**, 1715–1724.
3 M. O'Keeffe, M. A. Peskov, S. J. Ramsden and O. M. Yaghi, *Acc. Chem. Res.*, 2008, **41**, 1782–1789.
4 O. M. Yaghi, M. O'Keeffe, N. W. Ockwig, H. K. Chae, M. Eddaoudi and J. Kim, *Nature*, 2003, **423**, 705–714.
5 O. M. Yaghi, *J. Am. Chem. Soc.*, 2016, **138**, 15507–15509.
6 K. Otake, Y. Cui, C. T. Buru, Z. Li, J. T. Hupp and O. K. Farha, *J. Am. Chem. Soc.*, 2018, **140**, 8652–8656.
7 J. Lee, O. K. Farha, J. Roberts, K. A. Scheidt, S. T. Nguyen and J. T. Hupp, *Chem. Soc. Rev.*, 2009, **38**, 1450–1459.
8 D. Yang and B. C. Gates, *ACS Catal.*, 2019, **9**, 1779–1798.
9 C. Wang, B. An and W. Lin, *ACS Catal.*, 2019, **9**, 130–146.
10 J. A. Mason, M. Veenstra and J. R. Long, *Chem. Sci.*, 2013, **5**, 32–51.
11 S. Ma and H.-C. Zhou, *J. Am. Chem. Soc.*, 2006, **128**, 11734–11735.
12 D.-X. Xue, Y. Belmabkhout, O. Shekhah, H. Jiang, K. Adil, A. J. Cairns and M. Eddaoudi, *J. Am. Chem. Soc.*, 2015, **137**, 5034–5040.
13 L. E. Kreno, K. Leong, O. K. Farha, M. Allendorf, R. P. Van Duyne and J. T. Hupp, *Chem. Rev.*, 2012, **112**, 1105–1125.
14 C. A. Bauer, T. V. Timofeeva, T. B. Settersten, B. D. Patterson, V. H. Liu, B. A. Simmons and M. D. Allendorf, *J. Am. Chem. Soc.*, 2007, **129**, 7136–7144.
15 A. J. Howarth, Y. Liu, J. T. Hupp and O. K. Farha, *CrystEngComm*, 2015, **17**, 7245–7253.
16 R. J. Drout, L. Robison, Z. Chen, T. Islamoglu and O. K. Farha, *TRECHEM*, 2019, **1**, 304–317.
17 P. A. Kobielska, A. J. Howarth, O. K. Farha and S. Nayak, *Coord. Chem. Rev.*, 2018, **358**, 92–107.
18 P. Horcajada, C. Serre, G. Maurin, N. A. Ramsahye, F. Balas, M. Vallet-Regí, M. Sebban, F. Taulelle and G. Férey, *J. Am. Chem. Soc.*, 2008, **130**, 6774–6780.
19 C. Orellana-Tavra, R. J. Marshall, E. F. Baxter, I. A. Lázaro, A. Tao, A. K. Cheetham, R. S. Forgan and D. Fairen-Jimenez, *J. Mater. Chem. B*, 2016, **4**, 7697–7707.
20 N. L. Rosi, J. Kim, M. Eddaoudi, B. Chen, M. O'Keeffe and O. M. Yaghi, *J. Am. Chem. Soc.*, 2005, **127**, 1504–1518.
21 Y. Cui, Y. Yue, G. Qian and B. Chen, *Chem. Rev.*, 2012, **112**, 1126–1162.
22 Y. Cui, B. Li, H. He, W. Zhou, B. Chen and G. Qian, *Acc. Chem. Res.*, 2016, **49**, 483–493.
23 J. H. Cavka, S. Jakobsen, U. Olsbye, N. Guillou, C. Lamberti, S. Bordiga and K. P. Lillerud, *J. Am. Chem. Soc.*, 2008, **130**, 13850–13851.

24 H. Furukawa, F. Gándara, Y.-B. Zhang, J. Jiang, W. L. Queen, M. R. Hudson and O. M. Yaghi, *J. Am. Chem. Soc.*, 2014, **136**, 4369–4381.
25 J. E. Mondloch, W. Bury, D. Fairen-Jimenez, S. Kwon, E. J. DeMarco, M. H. Weston, A. A. Sarjeant, S. T. Nguyen, P. C. Stair, R. Q. Snurr, O. K. Farha and J. T. Hupp, *J. Am. Chem. Soc.*, 2013, **135**, 10294–10297.
26 J. Winarta, B. Shan, S. M. Mcintyre, L. Ye, C. Wang, J. Liu and B. Mu, *Crys. Growth Des.*, 2020, **20**, 1347–1362.
27 M. J. Katz, Z. J. Brown, Y. J. Colón, P. W. Siu, K. A. Scheidt, R. Q. Snurr, J. T. Hupp and O. K. Farha, *Chem. Commun.*, 2013, **49**, 9449–9451.
28 V. Quezada-Novoa, H. M. Titi, A. Sarjeant and A. Howarth, , DOI:10.26434/chemrxiv.12355406.v1.
29 S. Fordham, X. Wang, M. Bosch and H.-C. Zhou, in *Lanthanide Metal-Organic Frameworks*, ed. P. Cheng, Springer Berlin Heidelberg, Berlin, Heidelberg, 2014, vol. 163, pp. 1–27.
30 D.-X. Xue, A. J. Cairns, Y. Belmabkhout, L. Wojtas, Y. Liu, M. H. Alkordi and M. Eddaoudi, *J. Am. Chem. Soc.*, 2013, **135**, 7660–7667.
31 E. A. Dolgopolova, A. M. Rice and N. B. Shustova, *Chem. Commun.*, 2018, **54**, 6472–6483.
32 S. L. Hanna, X. Zhang, K. Otake, R. J. Drout, P. Li, T. Islamoglu and O. K. Farha, *Cryst. Growth Des.*, 2019, **19**, 506–512.
33 H. Jiang, J. Jia, A. Shkurenko, Z. Chen, K. Adil, Y. Belmabkhout, L. J. Weselinski, A. H. Assen, D.-X. Xue, M. O'Keeffe and M. Eddaoudi, *J. Am. Chem. Soc.*, 2018, **140**, 8858–8867.
34 D. J. Hoffart and S. J. Loeb, *Angew. Chem. Int. Ed. Engl.*, 2005, **44**, 901–904.
35 Y. He, H. Furukawa, C. Wu, M. O'Keeffe and B. Chen, *CrystEngComm*, 2013, **15**, 9328–9331.
36 D. T. de Lill and C. L. Cahill, *Chem. Commun.*, 2006, 4946–4948.
37 F. Serpaggi and G. Férey, *J. Mater. Chem.*, 1998, **8**, 2737–2741.
38 V. Kiritsis, A. Michaelides, S. Skoulika, S. Golhen and L. Ouahab, *Inorg. Chem.*, 1998, **37**, 3407–3410.
39 T. M. Reineke, M. Eddaoudi, D. Moler, M. O'Keeffe and O. M. Yaghi, *J. Am. Chem. Soc.*, 2000, **122**, 4843–4844.
40 H. He, D. Yuan, H. Ma, D. Sun, G. Zhang and H.-C. Zhou, *Inorg. Chem.*, 2010, **49**, 7605–7607.
41 J. S. Costa, P. Gamez, C. A. Black, O. Roubeau, S. J. Teat and J. Reedijk, *Eur. J. Inorg. Chem.*, 2008, 1551–1554.
42 R. Luebke, Y. Belmabkhout, Ł. J. Weseliński, A. J. Cairns, M. Alkordi, G. Norton, Ł. Wojtas, K. Adil and M. Eddaoudi, *Chem. Sci.*, 2015, **6**, 4095–4102.
43 D. F. Sava Gallis, L. E. S. Rohwer, M. A. Rodriguez, M. C. Barnhart-Dailey, K. S. Butler, T. S. Luk, J. A. Timlin and K. W. Chapman, *ACS Appl. Mater. Interfaces*, 2017, **9**, 22268–22277.
44 C. Liu, S. V. Eliseeva, T.-Y. Luo, P. F. Muldoon, S. Petoud and N. L. Rosi, *Chem. Sci.*, 2018, **9**, 8099–8102.
45 Ho-UiO-66 and Gd-UiO-66 were not activated, and their surface area was not measured.
46 R. A. Dodson, A. P. Kalenak and A. J. Matzger, *J. Am. Chem. Soc.*, 2020, **142**, 20806–20813.
47 N. Basma, P. L. Cullen, A. J. Clancy, M. S. P. Shaffer, N. T. Skipper, T. F. Headen and C. A. Howard, *Mol. Phys.*, 2019, **117**, 3353–3363.
48 B. Shan, S. M. McIntyre, M. R. Armstrong, Y. Shen and B. Mu, *Ind. Eng. Chem. Res.*, 2018, **57**, 14233–14241.
49 B. Bueken, N. Van Velthoven, A. Krajnc, S. Smolders, F. Taulelle, C. Mellot-Draznieks, G. Mali, T. D. Bennett and D. De Vos, *Chem. Mater.*, 2017, **29**, 10478–10486.
50 M. J. Cliffe, W. Wan, X. Zou, P. A. Chater, A. K. Kleppe, M. G. Tucker, H. Wilhelm, N. P. Funnell, F.-X. Coudert and A. L. Goodwin, *Nat. Comm.*, 2014, **5**, 4176.